

# Development of a web-based application for real-time eye disease classification system using artificial intelligence

Kennedy Okokpujie<sup>1,2</sup>, Adekoya Tolulope<sup>1</sup>, Abidemi Orimogunje<sup>3</sup>, Joshua Sokowonci Mommoh<sup>4</sup>,  
Adaora Princess Ijeh<sup>1</sup>, Mary Oluwafeyisayo Ogundele<sup>5</sup>

<sup>1</sup>Department of Electrical and Information Engineering, College of Engineering, Covenant University, Ota, Nigeria

<sup>2</sup>Africa Centre of Excellence for Innovative and Transformative STEM Education, Lagos State University, Ojo, Nigeria

<sup>3</sup>Department of Electrical and Electronic Engineering, Redeemer's University Ede, Ede, Nigeria

<sup>4</sup>Department of Software Engineering, Mudame University, Irrua, Nigeria

<sup>5</sup>Department of Cybersecurity, University of Delaware, Newark, United States

## Article Info

### Article history:

Received Sep 4, 2024

Revised May 28, 2025

Accepted Jun 10, 2025

### Keywords:

Convolution neural networks

Fundus images

MobileNetV3

ResNet-50

World Health Organization

## ABSTRACT

The incorporation of artificial intelligence (AI) into the field of medicine has created new strategies in enhancing the detection of disease, with a focus on the identification of eye diseases such as glaucoma, diabetic retinopathy, and macular degeneration associated with age, which can lead to blindness if not detected and treated early enough. Driven by the need to combat blindness, which affects approximately 39 million people globally, according to the World Health Organization (WHO). This research offers a web-based, real-time approach to classifying eye diseases from fundus images due to user-friendliness. Three pre-trained convolutional neural network (CNN) models are adopted, namely ResNet-50, Inception-v3, and MobileNetV3. The models were trained on a dataset of 8000 fundus images subdivided into four classes: cataract, glaucoma, diabetic retinopathy, and normal eyes. The performance of the models was evaluated in 3-way (normal eye and two diseases) and 4-way (normal eye and three diseases). ResNet-50 had higher performances, with 98% and 97% accuracy in the respective classifications, compared to InceptionV3 and MobileNetV3. Consequently, ResNet-50 was used in an online application that made real-time diagnoses. This research findings reveal the potential of CNNs in the healthcare industry, particularly in reducing over-reliance on specialists and increasing access to quality diagnostic technologies. Especially in critical areas such as this with limited healthcare resources, where the technology can create significant gaps in disease detection and control.

This is an open access article under the [CC BY-SA](https://creativecommons.org/licenses/by-sa/4.0/) license.



## Corresponding Author:

Kennedy Okokpujie

Department of Electrical and Information Engineering, College of Engineering, Covenant University

Km. 10 Idiroko Road, Canaan Land, Ota, Ogun State, Nigeria

Email: kennedy.okokpujie@covenantuniversity.edu.ng

## 1. INTRODUCTION

The rapid development of artificial intelligence (AI) in medicine has opened up new avenues to improve the accuracy and pace of disease diagnosis. Diabetic retinopathy, glaucoma, and age-related macular degeneration (AMD) are a few of the many such examples of eye disease diagnosis and have been one of the largest interests of many researchers. The diseases may result in severe visual impairment or blindness when diagnosed late, yet the diagnosis of eye diseases is usually dependent on expert opinion, utilization of expensive equipment, and longer diagnosis [1]. This is a great detriment to individuals residing in remote or poor regions with less accessibility to quality health facilities and experts. Hence, there is a growing need for

low-cost, portable, and scalable diagnostic technology that will be capable of identifying eye disease in real-time and allowing early intervention to prevent permanent loss of vision.

Eye disease is one of the prime reasons for blindness in the world, affecting millions of individuals, especially in third-world countries where health infrastructure is not available. A report from the World Health Organization (WHO) says that altogether, there are 39 million individuals throughout the world who are blind, and at least 2.2 billion individuals have near or distance vision deficiency. In at least 1 billion of them, vision loss can be prevented, so early and proper diagnosis is necessary to prevent vision loss [2].

Current methods for the detection of eye disease, especially in ophthalmology, rely on fundus imagery and optical coherence tomography (OCT) scanning. These imaging technologies present high-resolution images of the retina and optic nerve, which are crucial in diagnosing eye disease [3], [4]. Diagnosis of the images is usually left to the experts of ophthalmologists or imaging technicians. Manual inspection, however, is tedious, subjective, and error-prone. Moreover, it becomes infeasible in large-scale screening. Hence, an instant, automated, and scalable solution for eye disease detection from medical images is a pressing requirement.

Recent studies have shown that convolutional neural network (CNN)-based models, especially when trained from large annotated databases, can verify similar or even superior degrees of accuracy than human experts for the detection of diseases like diabetic retinopathy, glaucoma, macular degeneration, and retinal disease [5], [6]. High-profile systems such as DeepMind's AI diagnosis of eye disease have shown the capabilities of deep learning models to detect those diseases accurately from eye scans, usually detecting early signs that may go undetected by human physicians.

Three eye conditions, namely diabetic retinopathy, cataract and glaucoma, were selected for the study because of their prevalence in eye health all over the world. Cataracts can be seen as a medical condition where the eye lenses become hazy, and eyesight compromised. It is mostly caused by factors such as advancement in age, radiation, certain medications or even at-birth (congenital cataract) triggers. Symptoms and signs most typically reported with cataracts are night blindness, photophobia and glare, changing glasses or contact lens prescription, colour loss, and blurred vision [7]-[9]. Daily activities such as driving, reading, and recognizing people are negatively affected by cataracts, which decreases their quality of life. This accounts for blindness among elderly people worldwide. Cataracts are commonly treated by substitution with an artificial clear lens implant and surgical excision of the pacified lens. The procedure is indeed extremely safe and effective in most patients regaining good vision [10].

Glaucoma refers to a collection of eye problems that lead to optic nerve loss required for a clear sight. The condition is normally brought about by the excessively high pressure in the eye. It is the leading cause of blindness among persons older than sixty years. Glaucoma can be brought about by genetic problems, serious infections in the eyes, blocked eye blood vessels, or inflammatory diseases [11], [12]. Signs of developing glaucoma can be rather delicate at the onset but would usually include gradually progressive peripheral field loss, causing tunnel vision finally, then sudden pain in the eye, sometimes accompanied by nausea and vomiting, reddening of the eyes, sudden breaks into vision and halos encompassing light. Its impact on human life is quite large, and permanent vision loss occurs if treatment is not given adequately. Glaucoma can be treated using prescription eyedrops, oral medications, laser surgery, and other surgical means designed to lower intraocular pressure and prevent continuing optic nerve damage [13], [14].

Diabetic retinopathy is a diabetes-related eye disease. Data shows that eye disease causes damage to the blood vessels at the back part of the eye in a light-sensitive tissue known as the retina. Diabetic retinopathy can occur in any person who has diabetes—whether it's type 1 or 2—and the risk of developing it is greater the longer a person has diabetes and the less well it is controlled blood glucose levels. Diabetic retinopathy-floaters, blurry vision, fluctuating vision, dark or blank spots- which can feel like areas of blindness. The disease would lead to blindness if not managed. The existence of diabetic retinopathy in life is seen when one is hindered from reading, driving, or doing nearly everything else that requires good vision. Management and treatment focus on controlling blood sugar and blood pressure levels with laser surgery, vitrectomy, or drug injections into the eye to prevent further blood leakage from the vessels or any kind of inflammation. In addition, regular eye examinations are crucial for the early diagnosis and treatment of impending serious vision loss [15]-[17]. Recent research based on different deep-learning techniques for detecting eye diseases is discussed.

Siddique *et al.* [18] proposed an eye disease recognition model using CNNs. The research focused mainly on three eye diseases in Bangladesh, namely cataract, chalazion, and squint. Six CNN models, namely Xception, InceptionV3, DenseNet121, VGG16, VGG19, and MobileNet, were configured. After training, the MobileNet performed the other models with an accuracy of 97.49%. The model was not able to discern between a normal case and an eye disease.

Helen and Gokila [19] proposed an EYENET system for the detection of eye disease using CNNs. The EYENET model predicted five different eye disorders with strong prediction rates: glaucoma, cataracts,

uveitis, bulging eyes, and crossed eyes using a CNN, a self-diagnosis technique. The CNN architecture was efficient and improved disease prediction. The Adam optimizer was employed to optimize the proposed model. The evaluation metrics of precision, recall, accuracy, and F1-score are utilized to support the EYENET model. The maximum accuracy, 92.3%, was achieved by the EYENET model. However, the model was not deployed in real time to evaluate its performance in real-life scenarios.

Şüyun *et al.* [20] worked on the classification of hypertensive retinopathy based on the fundus images of patients of wide age using a deep learning approach. In order to train the deep learning model, additional data sets were produced based on Turkey and blended them with local data sets. The classified images were taken from only one imaging device. The data is to be integrated internationally, which can help standardize the results and increase accuracy. The method is used to identify retinal vascular degeneration, including macular edema and fundus vascular disease. The system achieved an area under curve (AUC) of 0.9622. All images used for the study were taken on a single device; the model may perform well on the images from that specific device but poorly on images taken from different devices or in different real-world conditions.

Glaret and Muthukannan [21] presented the use of an optimized CNN for the detection of multiple eye diseases. This paper proposed a method for the early detection of age-related eye diseases using retinal fundus images from the ocular disease intelligent recognition (ODIR) dataset. The images were pre-processed with maximum entropy transformation and then fed into a CNN for feature extraction. The CNN was optimized using a flower pollination optimization algorithm (FPOA) to enhance both accuracy and speed. Hyperparameters were also tuned through FPOA during training. The output from the CNN was subsequently classified using a multiclass support vector machine (MSVM). The proposed CNN-based multiple disease detection (CNN-MDD) model achieved outstanding performance, with precision, accuracy, specificity, recall, and F1-scores of 98.30%, 95.27%, 95.21%, and 93.3%, respectively, surpassing other optimized models. The developed model was not deployed.

Arif *et al.* [22] employed a CNN technique with EfficientNet architecture for the classification of fundus eye images. This study used EfficientNet-B0 for classification on a Kaggle dataset of 300 images. Data augmentation increased the dataset to 3,600 images, with 1,200 each for "normal," "cataract," and "glaucoma." Four datasets were generated: original, augmented, augmented grayscale, and augmented threshold images. With the Adam optimizer learning rate of 0.00001, batch size of 32, and 20 epochs, the augmented grayscale dataset showed accuracy, precision, recall, and F1-score of 79.22%, 80.3%, 79.22%, and 78.87%. However, the data augmentation process used can make data have unrealistic or deceptive variations, thereby reducing the ability of the model to generalize.

Du *et al.* [23] proposed an eye disease recognition system using a deep neural network for transfer learning with improved Dempster-Shafer (D-S) evidence theory. In the research, transfer learning was introduced to improve the deep learning-based eye recognition system and the efficiency of the model; the network was trained and fine-tuned. In order to eliminate the decision bias of the models and improve the credibility of the decisions, we propose a model decision fusion method based on the D-S theory. However, D-S theory is known to be incomplete and can lead to conflicting results, which may introduce decision paradoxes. To eliminate such limitations, we proposed a modified version of the D-S theory called the improved D-S evidence theory (ID-SET). The amendment was carried out to eliminate existing paradoxes and inconsistencies in the theory and hence enhance the reliability and accuracy of the decision fusion process. We applied ID-SET to the decision fusion of eye disease recognition models, demonstrating its effectiveness in improving the model's performance in terms of both decision consistency and trustworthiness. The developed model showed a significant reduction in inherent bias and improved robustness. The fused network achieved an accuracy of 0.9237, a Kappa of 0.878, an F1-score of 0.914 (95% CI [0.875–0.954]), a precision of 0.945 (95% CI [0.928–0.963]), a recall of 0.89 (95% CI [0.821–0.958]), and an AUC value of 0.987 for the ROC curve. The developed model was not deployed to see how the performance would be in a real-life setting.

Mangla *et al.* [24] proposed the use of a CNN for detecting ocular disease. The proposed system offered an economical and reliable approach for assisting in the early diagnosis of various diseases, including diabetes, glaucoma, cataracts, AMD, myopia, hypertension, and other related conditions. The model utilized the ODIR-2019 dataset, a structured ophthalmic database containing eye images along with demographic information, such as the ages of 5,000 patients. The annotations were performed by trained human readers to minimize errors caused by mislabeled data. Computer vision and deep learning techniques were leveraged to detect abnormalities in high-resolution fundus images. The proposed model was tested with various disease combinations, achieving a peak accuracy of 93% when applied to a single disease and an accuracy of 83% when used for diagnosing multiple diseases simultaneously. The dataset used only contained different eye disease cases without a normal case; hence, the model won't be able to discern between a normal case and an eye with the disease.

In general, the current techniques have performed greatly in the classification of eye diseases, but there have been a few limitations. One major gap (issue) is their inability to distinguish between normal and diseased eyes, often due to the absence of normal cases in the datasets used to train the models. In addition, such models are limited in practical deployment, and their performance would be impacted in real-world conditions. Finally, the majority of the models exhibited reduced accuracy in diagnosing multiple diseases simultaneously, suggesting that models would not perform optimally under complex, multi-class scenarios. This research comes with considerable advances towards overcoming such limitations.

- Deep CNN models such as ResNet-50, InceptionV3, and MobileNetV3 should be adopted to improve performance in complex, multi-class scenarios.
- Training of models with datasets which contain normal cases to be able to discern between a normal and a disease case.
- Incorporating web-based applications for real-time deployment.

The research structure is arranged as follows: section 2 explains in detail the suggested methodological arrangement. Section 3 gives a detailed explanation of the results and a detailed examination. Finally, section 4 concludes the research, synthesising the key findings and their significance.

## 2. RESEARCH METHOD

The full approach used in the development of a scalable web-based application for real-time eye disease classification using CNNs is discussed in this section. The developed model is summarized in the conceptual framework in Figure 1, from the data acquisition, image preprocessing, dataset split, loading pre-trained CNN models, model training and validation, model evaluation, and finally, model deployment.

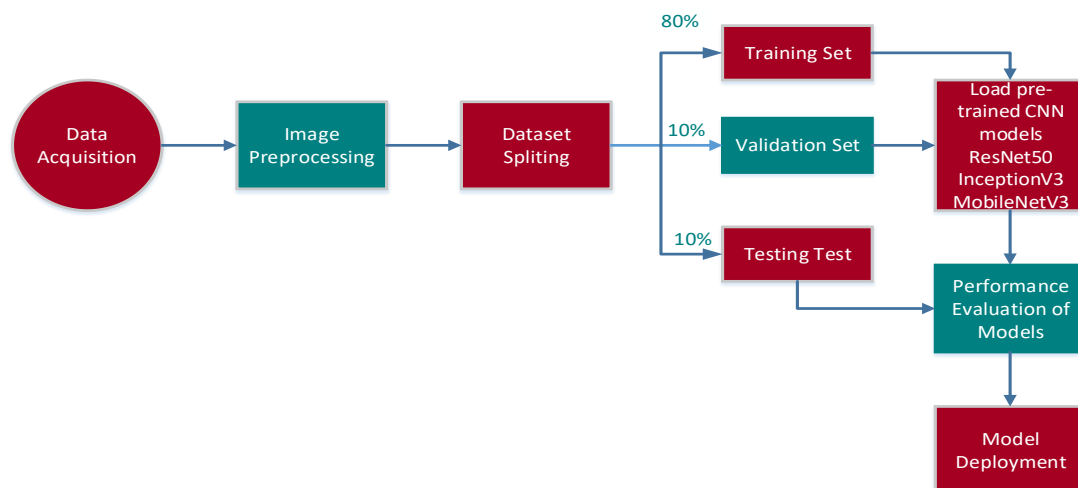


Figure 1. Conceptual framework

### 2.1. Dataset acquisition

The dataset used for this study was made of 8,000 images across four classes, namely, normal, cataract, glaucoma, and diabetic retinopathy. This dataset was formed from the combination of two distinct datasets. The first was the Chákṣu fundus image database, which consists of 1,345 retinal fundus images categorized into two classes, namely, normal eye images and glaucoma, retrieved from Figshare [25]. The second dataset was privately sourced, which included about 6,655 images divided into four classes, namely, normal eye images, cataract, glaucoma, and diabetic retinopathy. The two datasets were combined to create an improved dataset and a robust dataset size for better training of models to prevent the problem of generalization to unseen examples. Sample images from each class of image are depicted in Figure 2; also, various sizes of classes of the dataset are depicted in Table 1. The combined dataset averages 2000 images in each of the classes to handle the problem of unbalanced classes that could lead to biased training and poor generalization. Figure 2(a) shows an eye disease condition called glaucoma, while Figures 2(b) and (c) show that of cataracts and diabetic retinopathy, respectively, finally, Figure 2(d) shows the normal eye. Glaucoma is an eye ailment that damages the optic nerve [11], [12]. This impairment can lead to blindness. Cataracts are cloudy lenses that distress vision and can be instigated by ageing, injury, or other factors [7]-[9]. Diabetic

retinopathy is a diabetes complication that affects the eyes and is caused by a hurt to the blood vessels of the light-sensitive tissue at the retina (the back of the eye) [15]-[17].

Table 1. Groups of fundus images for the diseases

Disease (classes) type	No of images
Cataract	2000
Glaucoma	2000
Diabetic retinopathy	2000
Normal eye image	2000

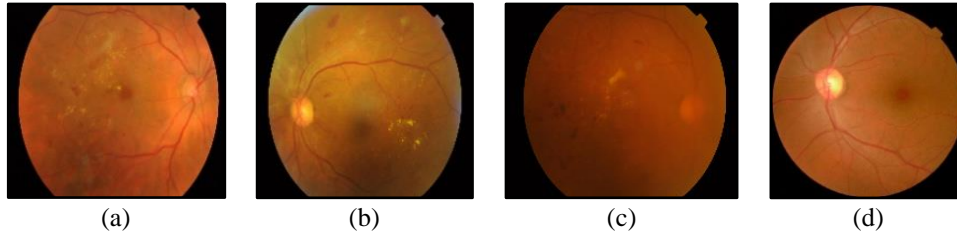


Figure 2. Sample of fundus images from the dataset with various eye conditions (a) glaucoma, (b) cataract, (c) diabetic retinopathy, and (d) normal eye

## 2.2. Image pre-processing

The image preprocessing phase consists of a series of key steps: cleaning of images, resizing, and normalisation. At the image cleaning stage, all the faulty, blurred, or incomplete images are removed from the dataset so that the model trains on high-quality data. It involves identifying and removing images with possible noise or irrelevant information, which might negatively impact model performance. Following this, the images are resized to the same dimensions in a way that they are consistent across the dataset. The transformation of pixel coordinates from the original image to the resized image is mathematically represented as (1) and (2):

$$x' = \frac{x}{W} \times W' \quad (1)$$

$$y' = \frac{y}{H} \times H' \quad (2)$$

where (x,y) are the original pixel coordinates and (x',y') are the coordinates after resizing, thereby making all images of the same size, which is a prerequisite for efficient batch processing and reduces computational burden during training. Normalization is the final step, where normalization is performed on the pixel values, bringing them into a common range, ranging from in between 0 and 1, so that the model is given inputs of the same intensity levels. It is done using min-max scaling, in which every original image pixel value p (between 0 and 255) is scaled as provided in (3):

$$P' = \frac{P}{255.0} \quad (3)$$

## 2.3. Dataset splitting

This research's dataset comprises a total of 8,000 images, equally divided into four classes with 2,000 images per class (cataract, glaucoma, diabetic retinopathy, and normal). To improve and generalize the model performance, the dataset was divided into a strategic split, that is, 80% for training for the model to learn from large data and understand all possible patterns for its categories. Furthermore, 10% was allotted for validation, which is used to monitor the model training performance. The validation set allows generalization and adjustment of hyperparameters during training. The last 10% was held out for the test set. It helps in giving an unbiased estimate of how well the model will perform after training and validation. Testing on unseen data will determine how the model carries out its performance and accuracy in annotating images for every category. The proportions of the data split are recorded in Table 2.

Table 2. Dataset split ratio

Classes	Training set (80%)	Validation set (10%)	Testing set (10%)
Cataract	1600	200	200
Glaucoma	1600	200	200
Diabetic retinopathy	1600	200	200
Normal eye image	1600	200	200
Total	6400	800	800

## 2.4. Model selection

Based on appropriate data preprocessing and subsequent division into training and validation/test datasets, three different CNN models were chosen and experimented with to gauge which model acted most favourably for eye disease classification within its own category. The three choices for our study were ResNet-50, InceptionV3, and MobileNetV3, which are all now considered state-of-the-art architectures in deep learning. ResNet-50, InceptionV3, and MobileNetV3 were selected for eye disease classification as they have been widely shown to efficiently extract subtle patterns in medical imaging. Training speed remains a strong point for ResNet-50; as a consequence of forming deeper networks and implementing residual connections, it now renders much faster training on large datasets. InceptionV3 excels in multi-scale feature extraction, which is of utmost importance in recognising subtle features in eye diseases. On the other hand, MobileNetV3, as a lightweight real-time on-device classifier, is extremely efficient and, therefore, well-suited for a web-based health application.

## 2.5. Model configuration

The inceptionV3 on the input resolution was 299×299, the ResNet-50 and MobileNetV3 were 224×224 pixels, which is a standard size for the majority of image classification issues, including medical image issues. The input resolution has a balance in that it collects enough image information without making computational demands too heavy. It allows the model to extract key features from eye fundus images, e.g., those that are suggestive of eye diseases like diabetic retinopathy or glaucoma, and maintain processing times within realistic bounds for actual applications in clinical scenarios. Pre-trained weights of ImageNet were utilized with all three models, which provided a substantial gain via transfer learning. ImageNet, a large dataset of over a million images distributed across a thousand categories, gives a consistent feature representation that can be quickly fine-tuned for other applications. By starting the models from these pre-trained weights, the network benefits from a strong foundation of learned features and can hence converge more quickly and attain better accuracy with fewer labelled images specialized for eye disease. This approach is particularly beneficial in medical imaging, where labelled retinal images are usually sparse and costly to obtain.

The layer count added at the end of the three architectures—ResNet-50, InceptionV3, and MobileNetV3—has been specially tuned for the specific task of eye disease classification, as shown in the pipeline Figure 3.

- a. Flatten layer: the Flatten() layer converts the multi-dimensional output from the convolutional base into a one-dimensional vector. This transition from convolutional layers to fully connected layers is essential for preparing the features extracted from retinal images for classification by the subsequent dense layers.
- b. dense layer (256 units, swish activation): the first dense (256, activation=swish) layer introduces 256 fully connected neurons with the swish activation function. Swish is a smooth, non-monotonic function defined by (4).

$$\text{Swish}(x) = x \cdot \text{sigmoid}(x) \quad (4)$$

The swish activation function makes the model more able to learn non-linear, subtle representations. This allows the model to capture subtle retinal image features, such as faint diabetic retinopathy, glaucoma, or cataract expressions.

- c. Dropout layer (50%): a dropout (0.5) layer is added as a regularization and overfitting prevention mechanism. This layer causes the model to perform well on new data by randomly zeroing 50% of the neurons during every training iteration, which is particularly crucial in medical imaging, where training sets are small.
- d. Dense layer (128 units, swish activation): the dense (128, activation=swish) layer is again utilized here to increase the ability of the model to learn from retinal images and detect more accurate eye disease complex patterns. Again, swish is used here because it can speed up learning in deep networks.
- e. Dropout layer (50%): another dropout (0.5) layer is included to maintain the regularization effect and avoid overfitting again as the model becomes deeper and learns increasingly abstract representations of eye disease features.

- f. Output layer: the output dense (K, activation="softmax", kernel\_regularizer=l2(0.001)) layer generates probability distributions over the K classes of the dataset (normal, diabetic retinopathy, glaucoma, cataract). Softmax activation ensures the output probabilities sum to one, making the model's class predictions interpretable. L2 regularization prevents overfitting by penalizing large weights, keeping the model robust and generalizable.

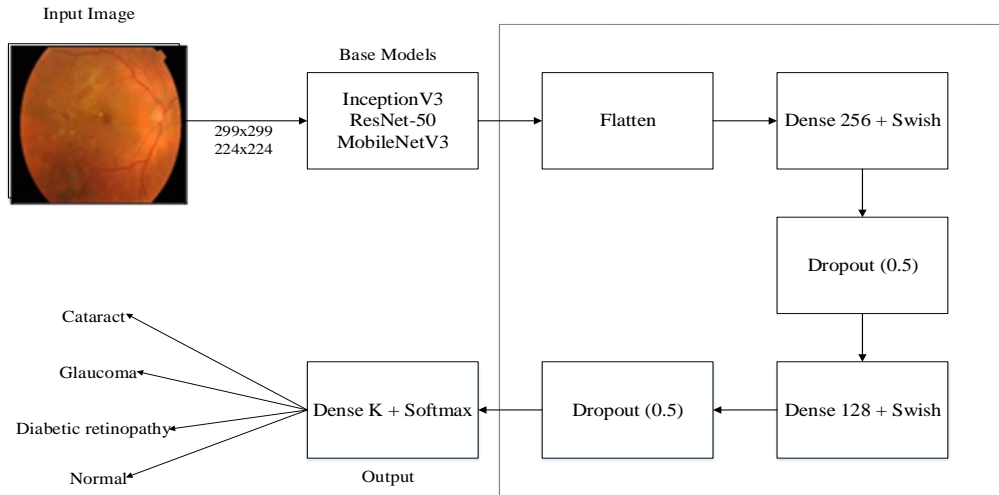


Figure 3. Transfer learning pipeline

This combination of layers has facilitated the model to extract key features from retinal images with speed and then accurately classify them. The swish activation function, dropout regularization, and L2 regularization on output layers improved the performance of models for the eye disease classification task in that regard.

The hyperparameters of Table 3 were the various configurations used to train the three variants of CNN adopted for this study. All three models made use of a categorical cross-entropy loss function, suitable for the multi-class classification. The models are trained by 32 batch sizes, which is the standard in memory efficiency and model convergence. All the models were trained at a fixed epoch of 20, allowing each model enough time to learn from the inputted data. Early stopping, with a patience of 3, avoids overfitting by shutting down training if validation loss does not drop for the subsequent three iterations. For the sake of a web application that scales to do real-time classification of eye disease, image size and model complexity are both important considerations to achieving optimal accuracy and processing speed. The InceptionV3 performs on comparatively larger images (299×299). While this may increase accuracy, it would become more computationally expensive, impacting the model's suitability for real-time applications on resource-constrained devices. In contrast, the 224×224 image resolution of MobileNetV3 and ResNet-50 is a compromise of model performance versus computational cost, hence their applicability to web applications where low latency is a key component for real-time predictions. All the models are ensured to be efficiently trained and converged owing to the Adam optimizer with a 0.001 learning rate, while training, validation, and test splits of 80:10:10 make sure proper training, validation, and testing have been done. All the above configurations allow for the performance optimization and accuracy of the models.

Table 3. Hyper parameters in the Rexnet-50, MobilenetV3, and Inceptionv3 models

Parameters	InceptionV3	MobileNetV3	ResNet-50
Image size	299×299	224×224	224×224
Batch size	32	32	32
Epochs	20	20	20
Patience	3	3	3
Learning rate	0.001	0.001	0.001
Optimizer	Adam	Adam	Adam
Loss function	Categorical cross-entropy	Categorical cross-entropy	Categorical cross-entropy
Training split	80%	80%	80%
Validation split	10%	10%	10%
Test split	10%	10%	10%
Callbacks	Early stopping	Early stopping	Early stopping

## 2.6. Model evaluation parametric

The confusion matrix was utilized to quantify the performance of the deep CNN model developed to predict eye diseases from fundus images. The performance of the model was quantified in terms of accuracy, precision, recall, and the F1-score for 4-way and 3-way eye disease classifications. Accuracy estimated the overall ratio of correct classifications, but this metric would be misleading if the dataset was unbalanced since some eye diseases could be more prevalent than others. Precision estimated the ratio of true positive predictions—i.e., identifying instances of a specific eye disease out of all positive predictions by the algorithm. Thus, this metric was pretty essential for reducing false positives, such as in the case of putting a healthy eye in the diseased category. Recall measured the model's ability to detect all true positive cases, which was extraordinarily important when the situation was such that missing a diagnosis of a disease (for example, glaucoma or diabetic retinopathy) had serious clinical ramifications. Finally, the F1-score attained an equal balance between precision and recall and was extremely useful in instances of skewed prevalence of diseases by category, which is typical in healthcare datasets. Such a measure guaranteed the web-based system for eye disease classification was accurate and trustworthy in real-time application in clinical environments. Mathematical expressions used for precision, accuracy, recall, and F1-score are given by (5)-(8) [26], [27]:

$$Accuracy = \frac{TP+TN}{TP+TN+FP+FN} \quad (5)$$

$$PPV = \frac{TP}{TP+FP} \quad (6)$$

$$Recall (TPR) = \frac{TP}{P} = \frac{TP}{TP+FN} \quad (7)$$

$$F1 = 2 \times \frac{PPV \times TPR}{PPV+TPR} \quad (8)$$

where: positive predictive value (PPV), true positive rate (TPR), false negative (FN), false positive (FP), and true positive (TP).

## 2.7. Development of web-based application

Adopting a user-friendly approach, this research developed a web-oriented application intending the real-time classification of eye diseases based on deep CNN models. The web interface developed on the Flask framework at the back end and HTML/CSS/JavaScript at the front end was meant for researchers uploading and classifying eye images into categories of different eye diseases such as cataracts, glaucoma, diabetic retinopathy, and normal status. The application provided a dynamic and responsive front end for the presentation of the classification outcomes in real-time. The phases were outlined as follows:

- Configuring the web interface: the web application began with Flask being used as the back-end framework to handle user requests and manage interactions with deep learning models. The front-end was created with HTML and CSS to create a responsive and clean layout. The layout included a middle file upload button to allow users to upload their eye images and a space to show the classification output.
- Uploading and displaying eye images: the upload image button gives the user access to upload an eye image from the personal workstation. A file dialogue will appear for the user to search and select the image he/she wants to classify. After choosing an image, resizing and pre-processing were done within the Pillow library. The image was shown on the web interface so the user could get a good look at it before classification.
- Displaying results of classification: the model output showed the predicted class of eye disease and was presented on the web interface, allowing users to easily identify what disease the model predicted.

## 2.8. System specification

The research was carried out on an HP Pavilion 15 laptop with an Intel Core™ i5-7200U processor (2.50 GHz, up to 2.71 GHz), 16 GB memory, and 256 GB SSD storage using the operating system Windows 10 Professional. The backend was done using Flask, and the frontend of a web-based application for real-time eye disease classification using CNN was done using HTML, CSS, and JavaScript. And Keras was used for building the models, Pillow and OpenCV for image processing. NumPy, Pandas, and Matplotlib took care of data manipulation and visualization, and SQLite was used to store metadata. Despite using these libraries, the lack of a GPU made it challenging to train the complex InceptionV3, MobileNetV3, and ResNet-50 models. More prolonged training hours resulted from the high image resolutions and high computational costs (299 times 299 pixels and 224 times 224 pixels) that the system with 16 GB RAM was working at full throttle during backpropagation and data splitting. This meant longer epochs; ultimately, the web application that could classify in real time was developed.



### 3. RESULTS AND DISCUSSION

All the chosen CNN models were well-trained, and their output was then visualized to check each one of them separately. Six models were derived from the chosen CNN architecture on the basis of training three-class and four-class datasets. Table 4 illustrates various CNN architectures and corresponding models for two classification problems: 3-class and 4-class. The table states three CNN architectures—ResNet-50, InceptionV3, and MobileNetV3—and their respective models for both classification tasks.

Table 4. CNN architectures with models

CNN models	3-class	4-class
Resnet-50	Model-1	Model-2
InceptionV3	Model-3	Model-4
MobilenetV3	Model-5	Model-6

For the 3-class classification task, ResNet-50 is referred to by Model-1, Model-3 refers to InceptionV3, and Model-5 refers to MobileNetV3. Also, for the 4-class classification task, ResNet-50 is referred to by Model-2, Model-4 refers to InceptionV3, and Model-6 refers to MobileNetV3.

#### 3.1. Resnet-50 (Model-1)

Figure 4 illustrates the training accuracy, validation accuracy, training loss, and validation of the ResNet 50 model-1 over 20 epochs in the training process. The training accuracy increases gradually and stabilizes, indicating that the model better fits the training data with the passage of time. The validation accuracy first increases peaks at epoch 10 and remains slightly fluctuating thereafter. This shows that the model does the best generalization to new data at epoch 10 but subsequently might overfit since training accuracy will continue to increase while validation accuracy will not. The training loss, which continuously decreases, shows that the model is learning and optimizing its fit to the training set. Also, the validation loss initially decreases and reaches its minimum at epoch 10. Subsequent to epoch 10, the validation loss starts to fluctuate and increase somewhat, showing that the model begins to overfit, capturing noise in the training set rather than patterns that are generalizable. This pattern is in agreement with the observation that epoch 10 offers the best trade-off between training and validation performance. All in all, model-1 (ResNet-50) was able to reach a training accuracy of 97% and a validation accuracy of 93%. Also, 0.2 training loss and 0.35 validation loss were achieved.

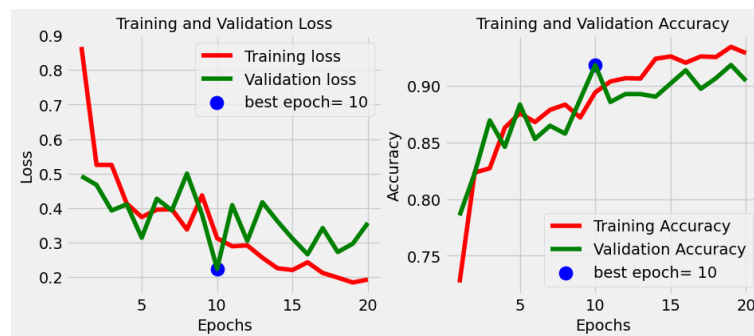


Figure 4. Training and validation loss and accuracy for Resnet-50 Model-1

#### 3.2. Resnet-50 (Model-2)

The graph in Figure 5 depicts training accuracy, validation accuracy, training loss, and validation loss for ResNet-50 (Model-2) after 20 epochs during training. The training accuracy continually increases and plateaus, i.e., the model improves at fitting the training data over time. The validation accuracy initially increases peaks at epoch 13 and fluctuates slightly afterwards. This pattern shows that the model is best on unseen data at epoch 13. Subsequently, while the training accuracy continues to improve, the validation accuracy does not, which is an indication of overfitting. The training loss continues to decrease steadily, indicating that the model is learning and improving at fitting the training data. The validation loss decreases initially and is lowest at epoch 12. Beyond epoch 12, the validation loss starts to fluctuate slightly but does not increase much, meaning mild overfitting, whereby the model starts to learn a bit of noise in the training

data instead of generalizable trends. This follows the fact that epoch 12 provides the best trade-off between training and validation performance. ResNet-50 (Model-2) achieved training accuracy, validation accuracy, training loss, and validation loss of 98%, 94%, 0.1, and 0.2, respectively.

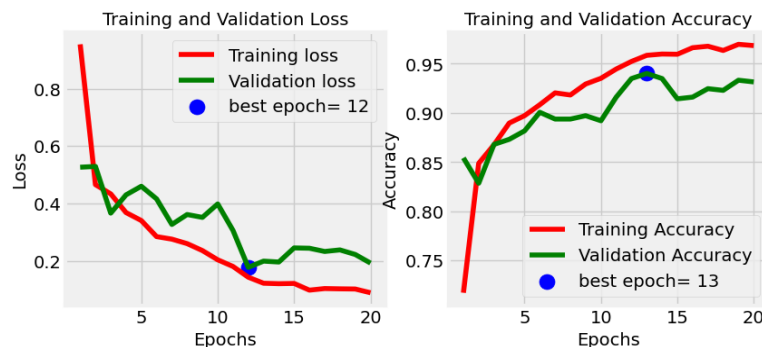


Figure 5. Training and validation loss and accuracy for Resnet-50 Model-2

### 3.3. InceptionV3 (Model-3)

Figure 6 illustrates the training accuracy, validation accuracy, training loss, and validation loss of InceptionV3 (Model-3). The training accuracy steadily increases, showing that the model improves its fit to the training data more and more as time passes. The validation accuracy initially rises and reaches a maximum around epoch 10, and this shows that this is the best-seen performance on unseen data. Following this, although training accuracy continues to improve, validation accuracy changes very slightly and no longer increase linearly, indicating an opportunity for overfitting. This type of pattern recognizes that epoch 10 provides the best trade-off between training and validation performance for the model in question so that generalization is very good with no indication of an overfitting tendency. Training loss, moreover, decreases monotonically, indicating the model learns well and improves too. Its suitability to the training data.

At the beginning, there is a decrease, and it continues to be the lowest point at epoch 10. Starting from then, the validation loss starts becoming highly spasmodic but never reaches the initial value, showing slight overfitting where the model tends to fill some information of the noise in the training data instead of generalizable patterns.



Figure 6. Training and validation loss and accuracy for InceptionV3 Model-3

### 3.4. InceptionV3 (Model-4)

InceptionV3 (Model-4) training accuracy, validation accuracy, training loss, and validation after 20 epochs during the process of training are shown in Figure 7. The training accuracy is growing slowly over time, showing that the model is adapting increasingly well to the training data. The training accuracy kept on increasing past epoch 12, but with regard to validation accuracy, there was no consistent improvement. This indicated some level of overfitting, where the model is learning patterns relying on only training data that falls short on new data. The validation loss was initiated high and soon dipped down to as low as possible at epoch 12—the pinnacle of model performance on unseen data. After more than epoch 12, validation loss

started to vary a little, showing some early signs of overfitting since the model now concentrates only on training data patterns instead of generalized characteristics. This is in comparison to the steadily decreasing training loss across all epochs, reflecting a better fit of the model to training data. This move confirms that epoch 12 gives the best balance between training and validation loss to allow for correct generalization without much overfitting. Overall, the InceptionV3 (Model-4) achieved training and validation accuracy of 93% and 86%, respectively, as well as training and validation loss of 0.2 and 0.5.

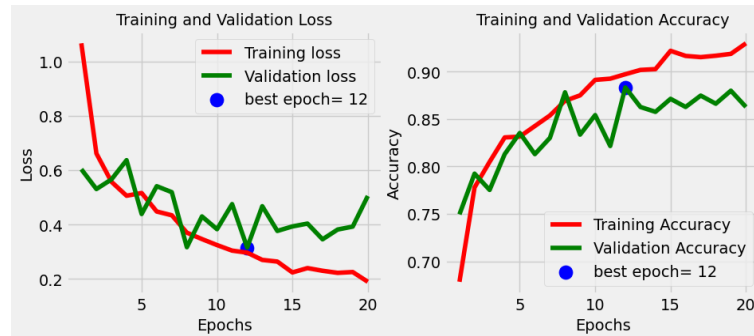


Figure 7. Training and validation loss and accuracy for Model-4

### 3.5. MobileNetV3 (Model-5)

From Figure 8, training accuracy consistently increases with epochs, demonstrating improvement in the model fitting the training data consistently. Validation accuracy rises and peaks at epoch 16, which is the best performance on new data at this point. With epoch 16 and beyond, although training accuracy continues to improve, validation accuracy begins to fluctuate, indicating potential overfitting where the model now learns noise rather than patterns that would generalize. This trend identifies epoch 16 as an epoch that provides an optimum trade-off between training and validation performance in generalization with no overfitting.

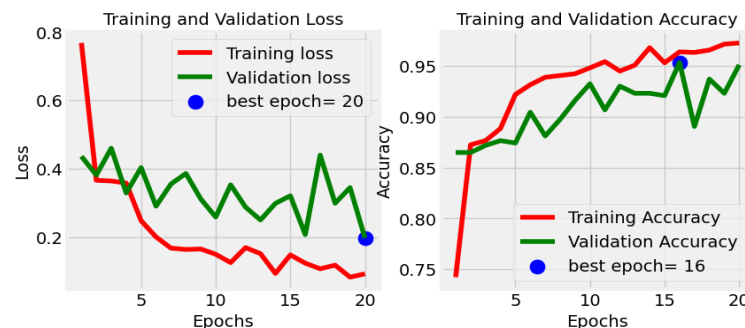


Figure 8. Training and validation loss and accuracy for MobileNetV3 (Model-5)

The training loss is still decreasing across epochs, meaning that the model continues to learn to fit the training data more effectively. The validation loss initially decreases but, after a few epochs, starts oscillating without a clear downward tendency, indicating the model's variable generalization performance on unseen data. It is found at epoch 20, the optimum epoch, and it reflects that this epoch offers the best relation between training performance and generalization ability before potential overfitting starts. The MobileNetV3 (Model-5) had a training accuracy and training loss of 98% and 0.2 and a validation accuracy and validation loss of 95% and 0.2, respectively.

### 3.6. MobileNetV3 (Model-6)

In Figure 9, it is observed that training accuracy increases consistently by epochs as a result of the persistent progress of the model in fitting the training data. Validation accuracy also increases and is at its peak at epoch 20, showing the best performance on unseen data here. While the training accuracy continues to rise, the validation accuracy is constant, which means that the model is generalizing well with no strong sign of overfitting. This performance suggests that epoch 20 provides the best compromise between training

and validation performance for good generalization. Besides, the training loss continues to decrease throughout the epochs, which means that the model is learning successfully and is improving its fit to the training data. Validation loss also decreases at first and is lowest at epoch 20, suggesting the best performance on unseen data at this epoch. Contrary to the overfitting trends seen before, validation loss does not vary or increase significantly after its minimum, suggesting good generalization. This trend aligns with the observation that epoch 20 gives the best balance between training and validation performance.

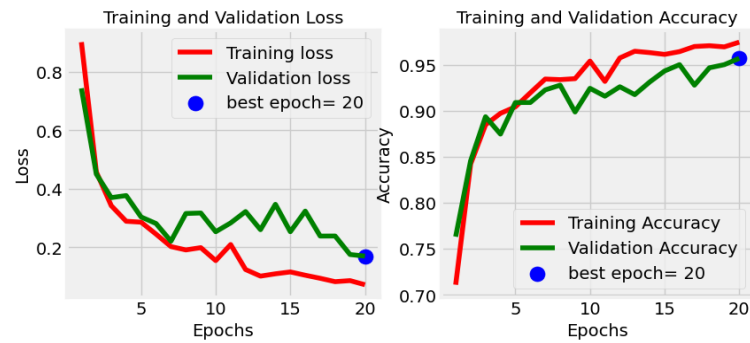


Figure 9. Training and validation loss and accuracy for MobiNetV3 (Model-6)

### 3.7. Models performance in terms of confusion matrices

A confusion matrix was used in terms of evaluating the performance of the classification models and obtaining better insight into their behaviour. It consists of two types of elements: diagonal and off-diagonal. Diagonal elements are those where the labels predicted were the same as the actual labels, i.e., accurate classification. A denser population diagonal suggests reduced misclassifications, while less populated off-diagonal values suggest fewer misclassifications.

On the other hand, the off-diagonal entries highlight where the classifier mislabelled or misclassified the data. A denser population diagonal suggests reduced misclassifications, while less populated off-diagonal values suggest fewer misclassifications. This makes the confusion matrix a rich source for making a complete report of the overall classification performance of the model for all classes. Figures 10–15 illustrate the ResNet-50 (Model-1 and Model-2), InceptionV3 (Model-3 and Model-4), and MobileNetV3 (Model-5 and Model-6) confusion matrices, offering an inclusive analysis of their performance.

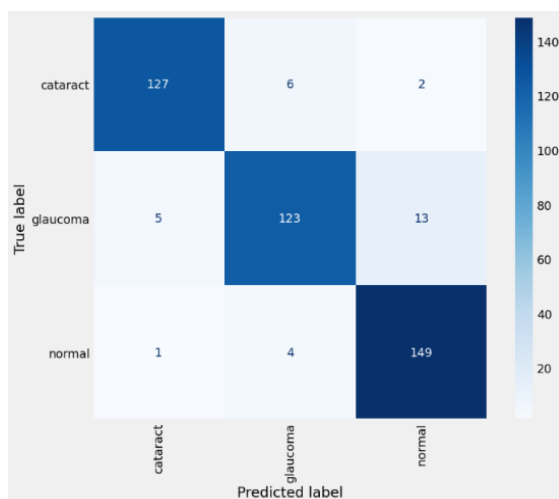


Figure 10. Confusion matrix for Model-1

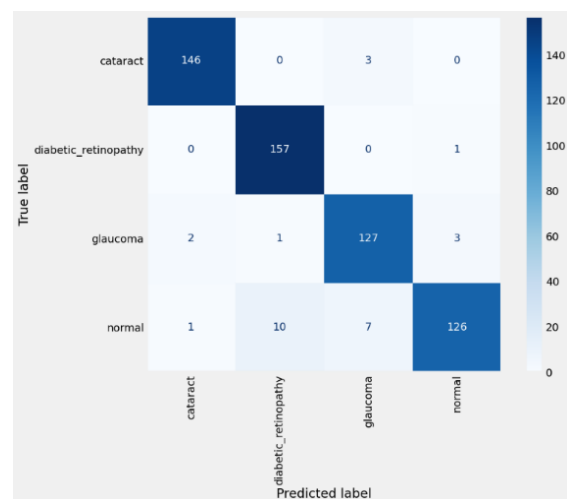


Figure 11. Confusion matrix for Model-2

The confusion matrix was central to evaluating the real-time eye disease classification model. It confirmed the capability of the model to identify specific eye diseases correctly and disclosed misclassification patterns among visually pertinent diseases, which offered useful insight into improving the CNN to perform more effectively.

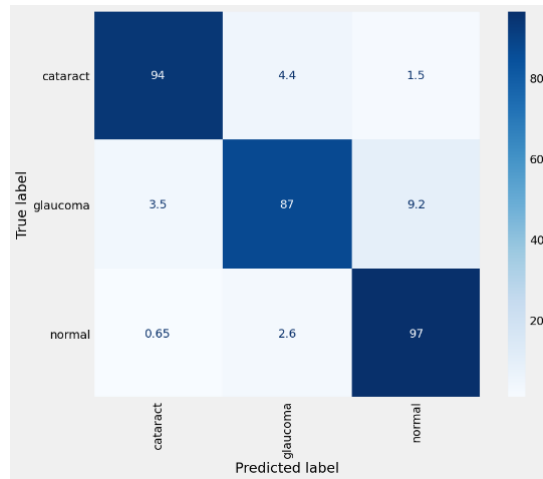


Figure 12. Confusion matrix for Model-3

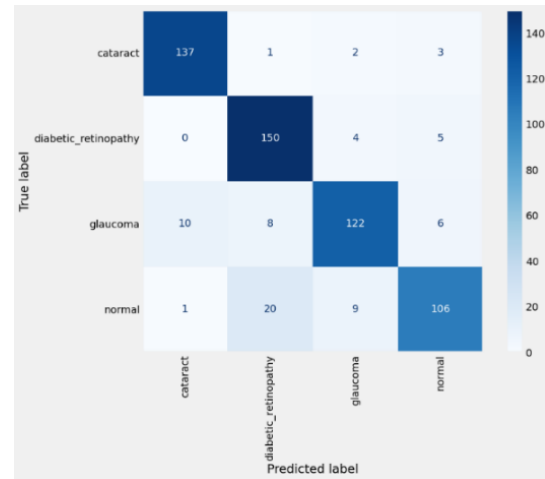


Figure 13. Confusion matrix for Model-4

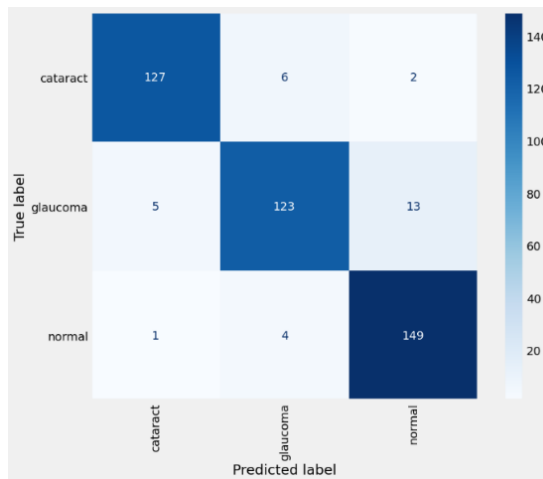


Figure 14. Confusion matrix for Model-5

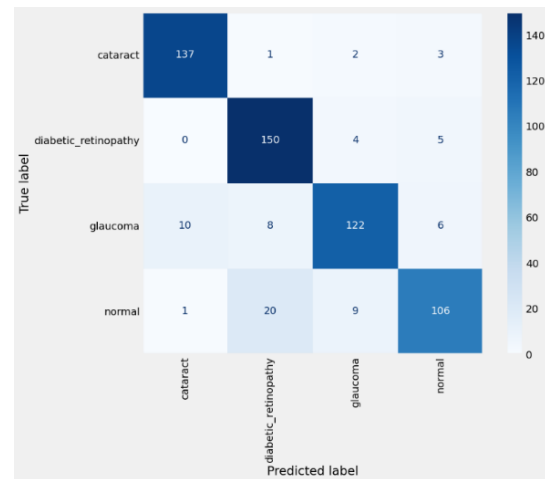


Figure 15. Confusion matrix for Model-6

### 3.8. Discussion

The performance is measured as classification accuracy, precision, F1-score, and recall of the three models (MobileNetV3, ResNet-50, and InceptionV3) for 3-class and 4-class eye disease classification is represented in Table 5. The findings highlight the performance of the models in relation to developing a scalable web-based application for real-time eye disease classification. MobileNetV3 does exhibit steady high performance, particularly being very effective in recall (99% for 3-class and 100% for 4-class), demonstrating its capability in precise identification of eye diseases. ResNet-50 and InceptionV3 are also good, with ResNet-50 exhibiting balanced values for the 4-class task (97% accuracy and 98% precision, F1-score, and recall) and InceptionV3 with slightly lower but comparable performance. All models were evaluated on 3-way and 4-way classification to see how performance varied as the size and class of the dataset increased.

Table 5. Average of performance results for the classes

Dataset type	Metrics	MobileNetV3 (%)	ResNet-50 (%)	InceptionV3 (%)
3-class	Accuracy	97	98	98
	Precision	97	95	95
	F1-score	98	95	95
	Recall	99	94	94
4-class	Accuracy	96	97	95
	Precision	97	98	93
	F1-score	98	98	94
	Recall	100	98	96

### 3.9. Model deployment

Here in this research, after the models were trained and tested, the ResNet-50 (Model-2) with four classes was used in the web-based application due to its performance as well as the number of classes in the dataset. Figure 16 illustrates an important aspect of the user interface and application workflow. This highlights the process from picture selection to their scan and ultimate prediction by the model, which is trained. Image selection, being the initial step, allows for the upload of eye images, typically captured through retinal scanning or similar technology, onto the web program. Once a picture is selected, the system is automatically switched to scan mode. At this point, the application pre-processes the picture, such as resizing and normalizing, so that it is in its right format. The real-time functionality of the application facilitates giving the results very fast so that healthcare professionals or patients can make sound decisions in time.

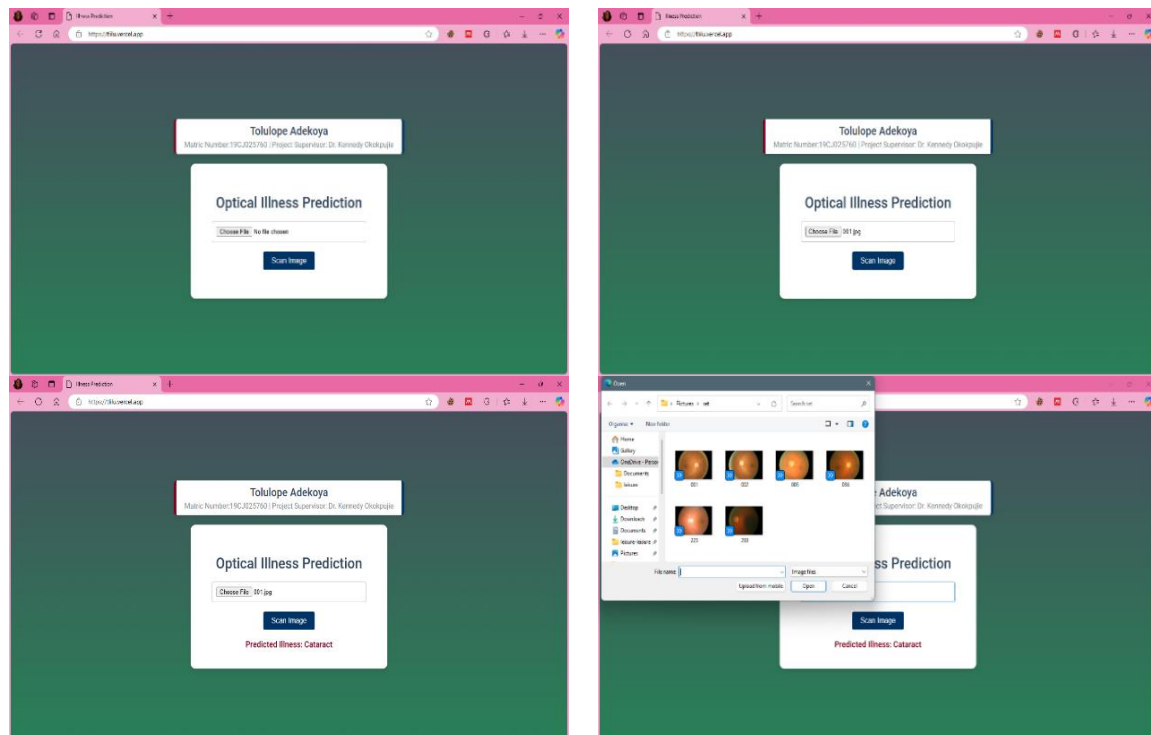


Figure 16. Images from web deployment

### 3.10. Comparative analysis

This section provides the comparative analysis of the deployed model with the closest related work in precision, recall, accuracy, F1-score, and deployment mode. Different classifiers' performance, such as the deployed model based on ResNet-50, is compared in Table 6. Among the provided models, the deployed model performs better in precision, recall, and F1-score, all of which are 98%, and accuracy is very high at 97%. In contrast to the previous high-performing model, MobileNet [18], with an accuracy of 97.49%, the presented model exhibits significantly improved precision (+2.79%), recall (+3.17%), and F1-score (+3.17%) and hence better control of both false positives and false negatives. Further, it outperforms ResNet [23] and VGG16 [28] in recall and F1-score, which are of most importance in sensitivity and specificity-demanding applications. EfficientB0 [22] falls significantly behind in all the metrics, so the developed model is an improvement. Besides performance, the deployment aspect also points to the practicality and usability of the developed model. In contrast to the other models, which have not been deployed, the developed ResNet-50 model is incorporated into a web application, making it more accessible and applicable in real-world scenarios. This deployment demonstrates the model's readiness for end-user adoption, a step ahead of theoretical improvements. In addition, with a dataset of size 8000, the proposed model enjoys an ideal trade-off between performance and computation and performs competitively compared to models trained from extremely large datasets like ResNet ([23]), which used 31,548 samples. Overall, the proposed model not only gains better evaluation metrics but is also useful in practice, hence an overall improvement over previous work.

Table 6. Comparative analysis of developed model with most recent related research

Author	Classifier	Dataset size	Evaluation metrics				Deployment
			Accuracy (%)	Precision (%)	Recall (%)	F1-score (%)	
Siddique <i>et al.</i> [18]	MobileNet	2201	97.49	95.21	94.83	94.83	No
Arif <i>et al.</i> [22]	EfficientB0	3600	79.22	80.30	79.22	78.87	No
Du <i>et al.</i> [23]	ResNet	31548	92.37	94.50	89	91.40	No
Dipu <i>et al.</i> [28]	VGG16	5000	97.23	96.73	93.76	95.22	No
Developed model	ResNet-50	8000	97	98	98	98	Web application

#### 4. CONCLUSION

Deep learning has quickly become a strong solution for detection and classification issues, with precise accuracy that has made it mainstream in the medical field. Despite this, investigating how to improve existing mechanisms for optimal detection and classification is a behemoth task for researchers. This paper presents a web-based real-time approach to the classification of eye disease from eye images, spurred by the need to minimise the impact of eye-related conditions that lead to the blindness of 39 million humans around the world. The research began with collecting eye image datasets of cataracts, glaucoma, diabetic retinopathy, and normal eyes. Then, the collected eye images were preprocessed by cleaning them and resizing them so that they were as needed for input sizes by the selected models. The three CNN pre-trained models, ResNet-50, Inception V3, and MobileNetV3, were exhaustively trained on the eye images in an attempt to determine the most effective model and a suitable model for eye disease classification. The performance evaluation findings revealed that ResNet-50 was the highest performing in both the 4-way and 3-way classifications with accuracies of 97% and 98%, respectively. In addition, after evaluation and training, the ResNet-50 4-way classification model was implemented in a web-based application because of its performance and the number of eye diseases that it could classify.

The findings of this research highlight the potential of CNNs for application in medicine, particularly in reducing reliance on experts and enabling increased access to high-quality diagnostic tools, particularly in resource-constrained environments. The method has the potential to dramatically enhance eye disease diagnosis using real-time facilities, providing invaluable assistance in scenarios where specialist ophthalmologists can be in short supply. Nevertheless, one main drawback of the present study is that it examined only a couple of eye diseases with a restricted dataset and that it was tested only on a web-based system. Follow-up studies need to focus on expanding the dataset with a broader cross-section of ethnic groups and demographic variables to enhance the generalizability and robustness of the model, and a rollout to a mobile app should be contemplated for offline accessibility and higher security reasons.

For future research, the authors suggest that the dataset be hybridised across all races and that data collection be increased for more specific improvements. Furthermore, increasing the number of eye diseases classified, exploring other deep learning architectures, and integrating mobile-based deployment could greatly advance the research in this area. Incorporating AI into the field of medicine, such as this developed model, would create new strategies for enhancing disease detection. These findings could enhance the detection and help in the early treatment of eye diseases such as glaucoma, diabetic retinopathy, and macular degeneration.

#### ACKNOWLEDGEMENTS

We thank Covenant University Centre for Research and Innovation and Development (CUCRID), located in Ota, Ogun State, Nigeria.

#### FUNDING INFORMATION

This work was funded by Covenant University Centre for Research and Innovation and Development (CUCRID).

#### REFERENCES




- [1] M. Alghamdi and M. Abdel-Mottaleb, "A Comparative Study of Deep Learning Models for Diagnosing Glaucoma from Fundus Images," *IEEE Access*, vol. 9, pp. 23894–23906, 2021, doi: 10.1109/ACCESS.2021.3056641.
- [2] World Health Organization, "Blindness and visual impairment," *World Health Organization Fact Sheets*, Oct. 2023. [Online]. Available: <https://www.who.int/news-room/fact-sheets/detail/blindness-and-visual-impairment>. (Accessed: 17-Jan-2024).
- [3] I. Laíns *et al.*, "Retinal applications of swept source optical coherence tomography (OCT) and optical coherence tomography angiography (OCTA)," *Progress in Retinal and Eye Research*, vol. 84, 2021, doi: 10.1016/j.preteyeres.2021.100951.
- [4] E. Midena, L. Frizziero, T. Torresin, P. T. Boscolo, G. Miglionico, and E. Pilotto, "Optical coherence tomography and color fundus photography in the screening of age-related macular degeneration: A comparative, population-based study," *PLoS One*, vol. 15, no. 8, 2020, doi: 10.1371/journal.pone.0237352.



- [5] S. Muchuchuti and S. Viriri, "Retinal Disease Detection Using Deep Learning Techniques: A Comprehensive Review," *Journal of Imaging*, vol. 9, no. 4, 2023, doi: 10.3390/jimaging9040084.
- [6] E. Mohamed and M. A. Marwa, "Deep learning-based classification of eye diseases using Convolutional Neural Network for OCT images," *Frontiers in Computer Science*, vol. 5, 2024, doi: 10.3389/fcomp.2023.1252295.
- [7] H. Hashemi *et al.*, "Global and regional prevalence of age-related cataract: a comprehensive systematic review and meta-analysis," *Eye*, vol. 34, no. 8, pp. 1357–1370, 2020, doi: 10.1038/s41433-020-0806-3.
- [8] M. S. Sheikh *et al.*, "Cataract and glaucoma detection based on Transfer Learning using MobileNet," *Heliyon*, vol. 10, no. 17, 2024, doi: 10.1016/j.heliyon.2024.e36759.
- [9] J. H. Zhang *et al.*, "A Systematic Review of Clinical Practice Guidelines for Cataract: Evidence to Support the Development of the WHO Package of Eye Care Interventions," *Vision (Basel)*, vol. 6, no. 2, 2022, doi: 10.3390/vision6020036.
- [10] M. K. Hasan *et al.*, "Cataract Disease Detection by Using Transfer Learning-Based Intelligent Methods," *Computational and Mathematical Methods in Medicine*, 2021, doi: 10.1155/2021/7666365.
- [11] D. F. Santos, "Classifying Glaucoma Using Machine Learning Techniques," *medRxiv*, 2023, doi: 10.1101/2023.05.02.23289378.
- [12] J. C. Lauren *et al.*, "Automatic detection of glaucoma via fundus imaging and artificial intelligence: A review," *Survey of Ophthalmology*, vol. 68, no. 1, 2023, doi: 10.1016/j.survophthal.2022.08.005.
- [13] G. V. Datta, S. R. Kishan, A. Kartik, S. G. Sai, and S. Gowtham, "Glaucoma Disease Detection Using Deep Learning," *Proceedings of the Fifth International Conference on Electrical, Computer and Communication Technologies (ICECCT)*, Erode, India, 2023, pp. 1–6, doi: 10.1109/ICECCT56650.2023.10179802.
- [14] S. Saha, J. Vignarajan, and S. A. Fros, "Fast and fully automated system for glaucoma detection using color fundus photographs," *Scientific Reports*, vol. 13, no. 18408, 2023, doi: 10.1038/s41598-023-44473-0.
- [15] J. Ogden, D. M. Lee, and H. Moradi, "Transfer Learning for Classification of Retinal Disease using Fundus Imaging," *Proceedings of the 2023 IEEE 11th International Conference on Healthcare Informatics (ICHI)*, pp. 510–512, 2023, doi: 10.1109/ICHI57859.2023.00087.
- [16] S. Qummar, F. G. Khan, G. Shah, S. Shamshirband, and Z. U. Rehman, "A Deep Learning Ensemble Approach for Diabetic Retinopathy Detection," *IEEE Access*, vol. 7, pp. 150530–150539, 2019, doi: 10.1109/ACCESS.2019.2947484.
- [17] D. Diksha and G. Gagandeep, "Machine Learning Based Classification for Diabetic Retinopathy Detection using Retinal Images," *Proceedings of the 2023 International Conference on Artificial Intelligence and Smart Communication (AISC)*, Greater Noida, India, 2023, pp. 1379–1382, doi: 10.1109/AISC56616.2023.10085442.
- [18] M. A. A. Siddique, J. Ferdouse, M. T. Habib, M. J. Mia, and M. S. Uddin, "Convolutional Neural Network Modeling for Eye Disease Recognition," *International Journal of Online and Biomedical Engineering (iJOE)*, vol. 18, pp. 115–130, 2022, doi: 10.3991/ijoe.v18i09.29847.
- [19] D. Helen and S. Gokila, "EYENET: An Eye Disease Detection System using Convolutional Neural Network," *Proceedings of the 2023 2nd International Conference on Edge Computing and Applications (ICECAA)*, Namakkal, India, 2023, pp. 839–842, doi: 10.1109/ICECAA58104.2023.10212139.
- [20] S. B. Şüyun, Ş. Taşdemir, S. Biliş, and A. Milea, "Using a deep learning system that classifies hypertensive retinopathy based on the fundus images of patients of wide age," *Traitement du Signal*, vol. 38, no. 1, pp. 207–213, Feb. 2021, doi: 10.18280/TS.380122.
- [21] P. S. Glaret and P. Muthukannan, "Optimized convolution neural network based multiple eye disease detection," *Computers in Biology and Medicine*, vol. 146, 2022, doi: 10.1016/j.combiomed.2022.105648.
- [22] Z. Arif, R. Y. N. Fu'adah, S. Rizal, and D. Ilhamdi, "Classification of eye diseases in fundus images using convolutional neural network (CNN) method with efficientNet architecture," *Jurnal Riset Tindakan Indonesia (JRTI)*, vol. 8, no. 1, pp. 125–131, 2023, doi: 10.29210/30032835000.
- [23] F. Du *et al.*, "Recognition of eye diseases based on deep neural networks for transfer learning and improved D-S evidence theory," *BMC Medical Imaging*, vol. 24, no. 19, 2024, doi: 10.1186/s12880-023-01176-2.
- [24] A. Mangla, S. Dhall, N. Gupta, S. Rastogi, and S. Yadav, "Ocular Disease Recognition Using Convolutional Neural Networks," *Advanced Computing: Proceedings of the 2022 IACC Conference*, vol. 1781, 2022, doi: 10.1007/978-3-031-35641-4\_3.
- [25] H. J. R. Kumar *et al.*, "Chakṣu: A glaucoma specific fundus image database," Figshare, 2023. [Online]. Available: [https://figshare.com/articles/dataset/Ch\\_k\\_u\\_A\\_glaucoma\\_specific\\_fundus\\_image\\_database/20123135](https://figshare.com/articles/dataset/Ch_k_u_A_glaucoma_specific_fundus_image_database/20123135). (Accessed: Mar. 21, 2024).
- [26] K. Okokpujie, I. P. Okokpujie, O. I. Ayomikun, A. M. Orimogunje, and A. T. Ogundipe, "Development of a Web and Mobile Applications-Based Cassava Disease Classification Interface Using Convolutional Neural Network," *Mathematical Modelling of Engineering Problems*, vol. 10, no. 1, pp. 113–120, 2023, doi: 10.18280/mmep.100113.
- [27] K. Okokpujie, S. John, C. Ndujiuba, and E. Noma-Osaghae, "Development of an Adaptive Trait-Aging Invariant Face Recognition System Using Convolutional Neural Networks," *Lecture Notes in Electrical Engineering: Information Science and Applications*, vol. 621, 2020, doi: 10.1007/978-981-15-1465-4\_41.
- [28] N. Dipu, S. Shohan, and K. M. A. Salam, "Ocular Disease Detection Using Advanced Neural Network Based Classification Algorithms," *Asian Journal for Convergence in Technology*, vol. 7, no. 2, pp. 91–99, 2021, doi: 10.33130/AJCT.2021v07i02.019.





## BIOGRAPHIES OF AUTHORS







**Dr. Kennedy Okokpujie**    holds a Bachelor of Engineering (B.Eng.) in Electrical and Electronics Engineering, Master of Science (M.Sc.) in Electrical and Electronics Engineering, Master of Engineering (M.Eng.) in Electronics and Telecommunication Engineering and Master of Business Administration (MBA), Ph.D. in Information and Communication Engineering, besides several professional certificates and skills. He is an Associate Professor in the Electrical and Information Engineering Department at Covenant University, Ota, Ogun State, Nigeria. He is a Nigerian Society of Engineers member and a Senior Member of the Institute of Electrical and Electronics Engineers (SMIEEE). His research areas of interest include biometrics, artificial intelligence, digital signal processing, and communication engineering. He can be contacted at email: [kennedy.okokpujie@covenantuniversity.edu.ng](mailto:kennedy.okokpujie@covenantuniversity.edu.ng).









**Miss. Adekoya Tolulope**     is a Covenant University, Ota, Ogun State, Nigeria graduate from the Department of Electrical and Information Engineering. She is currently interning at KPMG, where she continues to build her professional and technical expertise. During her undergraduate studies, she worked on several impactful projects, including developing a system for classifying eye diseases from fundus images using CNN, integrating artificial intelligence and medical imaging for enhanced diagnostics. Her research interests span the fields of medical engineering, artificial intelligence, and computer vision, with a particular focus on the application of machine learning in healthcare. She has demonstrated strong leadership and collaboration skills through her involvement in numerous academic and extracurricular activities. She is proficient in programming languages such as Python and MATLAB and is familiar with frameworks like TensorFlow and Keras. She is passionate about contributing to technological innovations that improve patient outcomes and is committed to pursuing advanced research and education in intelligent healthcare systems. She can be contacted at email: [tolulope.adekoya@stu.cu.edu.ng](mailto:tolulope.adekoya@stu.cu.edu.ng).







**Abidemi Orimogunje**     holds a Bachelor of Science degree (B.Sc.) in Electrical and Electronic Engineering and a Master of Science degree (M.Sc.) in Electrical and Electronic Engineering, both from the University of Ibadan, Nigeria. He is a lecturer at the Redeemer's University, Ede, Nigeria. He is a member of the Institute of Electrical and Electronics Engineers (IEEE) and the Nigerian Society of Engineers (NSE). Currently, he is pursuing his Ph.D. program at the African Centre of Excellence in internet of things (ACEIoT), University of Rwanda, Kigali. His research interests include digital signal processing, machine learning, wireless communication, 5G and beyond 5G, internet of things, and electronic design. He can be contacted at email: [orimogunjea@run.edu.ng](mailto:orimogunjea@run.edu.ng).







**Joshua Sokowonci Mommoh**     holds a Bachelor of Engineering (B.Eng.) in Electrical Electronics Engineering and a Master of Engineering (M.Eng.) in Electronic and Communications Engineering. He is lecturing with the Department of Software Engineering at Mudiame University, Irrua, Edo State, Nigeria. His research areas of interest include machine learning, embedded systems, signal processing, and wireless sensor networks. He can be contacted at email: [mommoh.joshua@mudiameuniversity.edu.ng](mailto:mommoh.joshua@mudiameuniversity.edu.ng).



**Adaora Princess Ijeh**     is a postgraduate student currently pursuing a Master's degree in Computer Science. She holds a Bachelor's degree in Computer Science from the Federal University of Petroleum Resources, Effurun, Delta State, Nigeria. For her undergraduate research, she developed a web-based electronic management application to improve administrative efficiency. Her current research interests include cybersecurity and artificial intelligence, focusing on developing smart, data-driven systems. She is dedicated to advancing intelligent technologies through secure and innovative software solutions. She aspires to contribute to cutting-edge research in intelligent systems and secure software design, with the long-term goal of enhancing digital infrastructure in developing and developed regions. She can be contacted at email: [adaora.ijehpgs@stu.cu.edu.ng](mailto:adaora.ijehpgs@stu.cu.edu.ng).



**Mary Oluwafeyisayo Ogundele**     holds a B.Sc. in Electronics and Computer Engineering, a master's degree in information technology and a Master of Business Administration (MBA), amongst other professional certifications. She currently leads the Network and User Administration Team at Unified Payments Systems, a prominent fintech organisation in Nigeria. She served at Nigeria's Apex Bank, where she was responsible for administering and managing critical network and security solutions. She is a member of the Nigerian Society of Engineers (NSE), Council for the Regulation of Engineering in Nigeria (COREN) and a fellow of the National Institute of Professional Engineers and Scientists (NIPES). She is pursuing her Ph.D. at the University of Delaware in the Cybersecurity Department in Newark, Delaware, United States. She can be contacted at email: [maryo@udel.edu](mailto:maryo@udel.edu).